CHEMISTRY
A EUROPEAN JOURNAL

DOI: 10.1002/chem.201002522

Complexation Equilibria Involving Salts in Non-Aqueous Solvents: Ion Pairing and Activity Considerations

Harry W. Gibson,*[a] Jason W. Jones,[a, b] Lev N. Zakharov,[c, d] Arnold L. Rheingold,[c, e] and Carla Slebodnick[a]

Abstract: Complexation of anions, cations and even ion pairs is now an active area of investigation in supramolecular chemistry; unfortunately it is an area fraught with complications when these processes are examined in low polarity organic media. Using a pseudorotaxane complex as an example, apparent K_{a2} values ($=$[complex]/{[salt]$_o$−[complex]}-{[host]$_o$−[complex]}) for pseudorotaxane formation from dibenzylammonium salts (**2**-X) and dibenzo-[24]crown-8 (**1**, DB24C8) in $CDCl_3/CD_3CN$ 3:2 vary with concentration. This is attributable to the fact that the salt is ion paired, but the complex is not. We report an equilibrium model that explicitly includes ion pair dissociation and is based upon activities rather than molar concentrations for study of such processes in non-aqueous media. Proper analysis requires both a dissociation constant, K_{ipd}, for the salt and a binding constant for interaction of the free cation $\mathbf{2}^+$ with the host, K_{a5}; K_{a5} for pseudorotaxane complexation is independent of the counterion ($500\,M^{-1}$), a result of the complex existing in solution as a free cation, but K_{ipd} values for the salts vary by nearly two orders of magnitude from trifluoroacetate to tosylate to tetrafluoroborate to hexafluorophosphate anions. The activity coefficients depend on the nature of the predominant ions present, whether the pseudorotaxane or the ions from the salt, and also strongly on the molar concentrations; activity coefficients as low as 0.2 are observed, emphasizing the magnitude of their effect. Based on this type of analysis, a method for precise determination of relative binding constants, K_{a5}, for multiple hosts with a given guest is described. However, while the incorporation of activity coefficients is clearly necessary, it removes the ability to predict from the equilibrium constants the effects of concentration on the extent of binding, which can only be determined experimentally. This has serious implications for study of all such complexation processes in low polarity media.

Keywords: crown compounds · inclusion compounds · ion pairs · supramolecular chemistry

Introduction

The field of supramolecular chemistry has experienced an explosive growth over the past few decades,[1] and the past decade has seen the application of non-covalent chemistry to such diverse areas as sensors, molecular electronics, and molecular machines.[2] Charged species have played a dominant role in modern supramolecular chemistry, dating to Pedersen's discovery of the alkalai metal templated formation of crown ethers.[3] Indeed the study of "anion binding"[4] and "cation binding",[5] the latter mainly focused on ammonium salts because of their biological importance and pH sensitivity, continues unabated.

To tune potential applications, there exists a strong need to predict and control the reversible interactions that are the basis of supramolecular chemistry. As a result, a number of experimental methods have been reported to measure association constants, including calorimetry and various spectroscopic measurements.[6] Many of these techniques are cross-over technologies from the biological sciences and basically employ Equation (1).

$$H + G \overset{K_{a1}}{\rightleftharpoons} HG$$

$$K_{a1} = [HG]/[H][G] = [HG]/([H]_o - [HG])([G]_o - [HG]) \qquad (1)$$

However, the biological models and Equation (1) are intended for use with aqueous solutions, whereas many synthetic complexes are studied in low dielectric constant organic media in order to avoid H-bonding competition. While solvent/complex interactions are minimized in low di-

[a] Prof. Dr. H. W. Gibson, Dr. J. W. Jones, Dr. C. Slebodnick
Department of Chemistry, Virginia Polytechnic Institute and State University, Blacksburg, VA 24061-0212 (USA)
E-mail: hwgibson@vt.edu

[b] Dr. J. W. Jones
Present address:
E.I. duPont de Nemours and Company
Wilmington, DE 19880-0402 (USA)

[c] Dr. L. N. Zakharov, Prof. Dr. A. L. Rheingold
Department of Chemistry, University of Delaware
Newark, DE 19716 (USA)

[d] Dr. L. N. Zakharov
Present address:
X-ray Crystallography Facility
University of Oregon, Eugene, Oregon 97403 (USA)

[e] Prof. Dr. A. L. Rheingold
Present address:
Department of Chemistry and Biochemistry
University of California, San Diego, La Jolla, CA 92093 (USA)

electric solvents, so too are solvent/ion interactions: as a result, ion pair formation is known to occur.[7] This has often been ignored[8] in host/guest studies of salts in low dielectric constant media.

In such cases there are at least four extreme situations that may occur, as outlined below. First, both the guest salt and the complex may be ion paired:

$$H + G^+X^- \overset{K_{a2}}{\rightleftharpoons} HG^+X^-$$

$$K_{a2} = [HG^+X^-]/[H][G^+X^-] = [HG^+X^-]/([H]_o - [HG^+X^-])([G^+X^-]_o - [HG^+X^-]) \quad (2)$$

Second, the guest salt and the complex may be completely ionized, that is, not ion paired:

$$G^+X^- \rightarrow G^+ + X^-$$

$$H + G^+ \overset{K_{a3}}{\rightleftharpoons} HG^+$$

$$K_{a3} = [HG^+]/[H][G^+] = [HG^+]/([H]_o - [HG^+])([G^+X^-]_o - [HG^+]) \quad (3)$$

Third, the guest salt could be completely ionized and the complex ion paired:

$$G^+X^- \rightarrow G^+ + X^-$$

$$H + G^+ + X^- \overset{K_{a4}}{\rightleftharpoons} HG^+X^-$$

$$K_{a4} = [HG^+X^-]/[H][G^+][X^-] = [HG^+X^-]/([H]_o - [HG^+X^-])([G^+X^-]_o - [HG^+X^-])^2 \quad (4)$$

Fourth, the guest salt could be ion paired and the complex fully ionized:

$$G^+X^- \overset{K_{ipd}}{\rightleftharpoons} G^+ + X^-$$

$$H + G^+ \overset{K_{a5}}{\rightleftharpoons} HG^+$$

$$H + G^+X^- \overset{K_{o5}}{\rightleftharpoons} HG^+ + X^-$$

$$K_{o5} = K_{ipd}K_{a5} = [HG^+][X^-]/[H][G^+X^-] = [HG^+][X^-]/([H]_o - [HG^+])[G^+X^-] \quad (5)$$

Note that in all cases except the latter, the equilibria can be evaluated simply by NMR spectroscopy because all of the concentrations can be directly determined. However, in the last case, note that in Equation (5) there is no direct way to determine the concentration of either the free counterion X^-or the ion paired salt G^+X^-under ordinary circumstances, that is, in the absence of knowledge of K_{ipd}. Because of the ion pair dissociation equilibrium the concentrations of three species, G^+, $X^-$and G^+X^-, are not simply related to the original concentration of guest salt and the concentration of complex.

The well studied pseudorotaxane[9] formed from dibenzo-[24]crown-8 (**1**) and dibenzylammonium salts (**2**-X) (Scheme 1)[10] is an ideal candidate for complexation studies because exchange is slow on the NMR time scale: in addition to peaks associated with the starting compounds, new signals corresponding to complex formation (**1·2**-X) are readily discerned; by integration, the complex stoichiometry (1:1) and concentration may be readily determined.

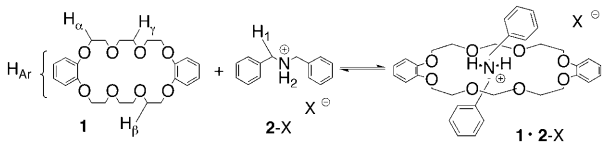

Scheme 1. Formation of pseudorotaxane complex from dibenzo-[24]crown-8 (**1**) and dibenzylammonium salts (**2**-X).

Considering the process in Equation (2) [or equivalently Eq. (3)] by the procedure used generally in the literature, the concentration of the complex, $[HG^+]$, can be measured and the concentration of the uncomplexed salt, $[G^+X^-]$, is assumed to be $[G^+X^-]_0 - [HG^{+-}]$ and $[H] = [H]_0 - [HG^+]$. We examined the formation of pseudorotaxane **1·2**-X by ^{1}H NMR spectroscopy over a range of starting host and guest concentrations at 295 K in $CDCl_3/CD_3CN$ 3:2 (by volume).[11] Several important facts were revealed: 1) the concentration based K_{a2} values according to Equation (2) [or K_{a3} via Eq. (3)] varied strongly with a) host concentration and b) salt concentration; 2) the chemical shifts attributed to the pseudorotaxane were invariant with concentration and anion (Figure 1), whereas the chemical shifts attributed to uncomplexed guest salt **2**-X changed with concentration and were dependent on the anion.[11,12]

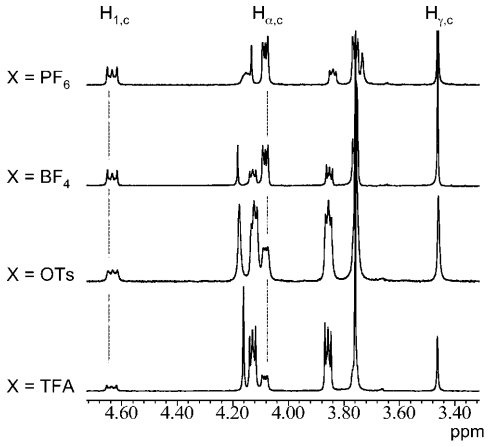

Figure 1. Partial 400 MHz ^{1}H NMR spectra of DB24C8 (**1**, 4.00 mM) and dibenzylammonium salts (**2**-X, 4.00 mM) with various counterions in$CD_3CN/CDCl_3$ 2:3 at 22 ± 1 °C. The signals of protons in the pseudorotaxane are indicated by subscript "c". OTs = tosylate anion. TFA = trifluoroacetate anion. The same chemical shifts for the pseudorotaxane complex were observed with **1** and **2**-OTf (triflate = trifluoromethanesulfonate); see Supporting Information.

We, therefore, concluded that Equation (2) (or 3) does not obtain in the formation of these pseudorotaxanes from dibenzo-[24]crown-8 in low polarity solvents at concentrations used in NMR analyses, typically 1 to 10 mM; in these cases the guest is entrapped in the small cavity of the host in such a way that ion pairing of the complex does not occur.[13] To evaluate these equilibria, we proposed data treatments that used Equation (5) with approximations of the concentrations of the counterion $X^-$and guest salt G^+X^-. Here we describe a more rigorous approach to analysis of such systems and introduce guidelines for detection of this situation, which we believe occurs more widely than presumed.

Results and Discussion

Effect of solvent: In our prior work we used the 2:3 (v/v) $CD_3CN/CDCl_3$ solvent system and showed that **2**-TFA had a low ion-pair dissociation constant therein.[11] Figure 2 displays spectra of **1** and **2**-TFA taken in $CDCl_3$. Note that no new signals appear; the crown ether protons remain essentially unchanged, as do the guest signals, with up to a 21-fold excess of the latter. We conclude that in $CDCl_3$ the guest salt is essentially totally ion paired and hence does not interact with the crown ether.

On the other hand in $CD_3CN/CDCl_3$ 2:3, complex **2**-PF_6 possesses a relatively high ion-pair dissociation constant.[11] In the present work we examined **1** and **2**-PF_6 in [D_6]acetone. Indeed, over a range of concentrations (2 to 16 mM in **1** and 2 to 16 mM in **2**-PF_6, see Supporting Information) in this solvent the complexation of guest **2**-PF_6 by dibenzo-[24]crown-8 (**1**) seems to follow the scenario described by Equation (3) above. That is, K_{a3} is constant within experimental error: $K_{a3}=418\pm41\,M^{-1}$ (10 data points) for extents of complexation between 10 and 90% (near the Weber rule range of 20–80% complexation[14]); Stoddart et al. reported $K=360\,M^{-1}$ in this solvent by a single measurement at unspecified concentrations.[15] The apparent lack of concentration dependence is attributed to the higher polarity of acetone (ε = 20.7) vs. 2:3 (v/v) $CD_3CN/CDCl_3$ (ε estimated to be 17.5 by volume averaging), thus allowing most of the guest **2**-PF_6 to be predominantly ionized and the ammonium cation to be captured by the crown ether guest as a non-ion paired complex, making Equation (3) a good approximation. Indeed there is evidence that in mixed solvents selective solvation influences ion pairing in a non-linear manner;[16] this may explain the large effect observed for a relatively small change in bulk dielectric constant from acetone to $CD_3CN/CDCl_3$ 2:3. (Note: these results were derived from spectra recorded immediately after solution preparation, thus avoiding the complication that results when the ammonium salt reacts with the solvent.[17])

Effect of concentrations: In continuation of our previous work in $CD_3CN/CDCl_3$ 2:3, we varied the equimolar concentrations of **1** and **2**-PF_6 from 1 to 50 mM. A plot of K_{a2} (or equivalently K_{a3}) versus concentration resulted in a curve that approached an asymptotic limit of $K_{a2}=4.5\times10^2\,M^{-1}$ (Figure 3). The same asymptotic behavior was found with **1** and **2**-BF_4, but with a limit of $K_{a2}=1.3\times10^3\,M^{-1}$ (see Supporting Information). And with **1** and **2**-TFA the limiting value was ~20 M^{-1} (see Supporting Information).

Effect of added counterions: At constant equimolar concentrations (3.00 mM) of DB24C8 and **2**-PF_6 in $CD_3CN/CDCl_3$ 2:3 tetrabutylammonium TFA (TBA-TFA) was added in increasing concentrations; at TBA-TFA concentrations $\geq$ ~15 mM no detectable complexation occurred. This is the result of the strong ion pairing of **2**-TFA. (We demonstrated by ^{1}H NMR that TBA-TFA does not interact with the crown ether; see Supporting Information). In the X-ray crystal structure of the DBA-TFA salt (Figure 4) each carboxylate hydrogen bonds with an N-H proton on two proximal cations. The tosylate salt in the crystalline phase also forms a hydrogen bonded linear structure (Figure 5), while the triflate exists as a tetramer composed of two cations and two anions (Figure 6). In solution similar interactions presumably take place.

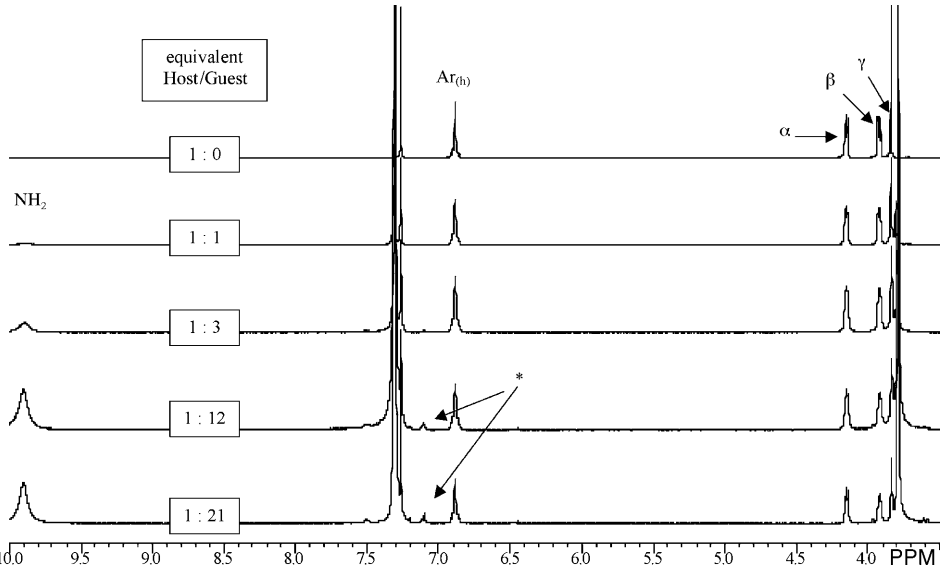

Figure 2. ^{1}H NMR spectra (400 MHz, 22.1 °C, $CDCl_3$) of solutions of DB24C8 (**1**, 3.5 mM) with (from top to bottom) 0, 1, 3, 12 and 21 equivalents of **2**-TFA. Solvent/guest impurities are labeled with *.

In a related study, [**1**] and [**2**-PF_6] were both held constant at 1.67 mM and tetrabutylammoni-

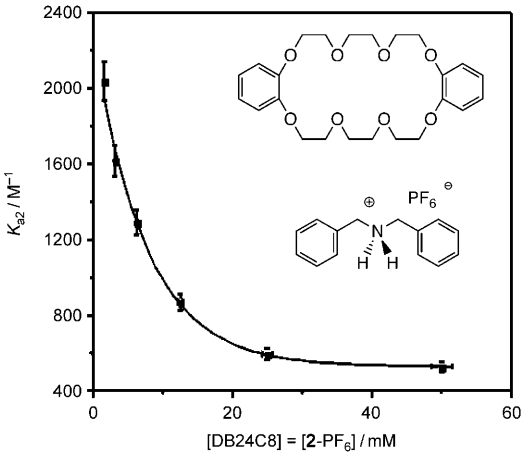

Figure 3. Variation of K_{a2} with equimolar concentrations of DB24C8 and **2**-PF_6 in $CD_3CN/CDCl_3$ 2:3 at 22 °C.

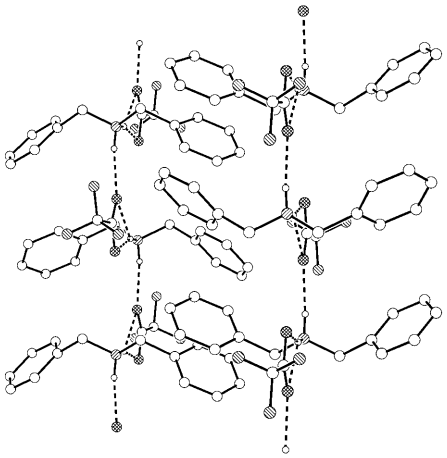

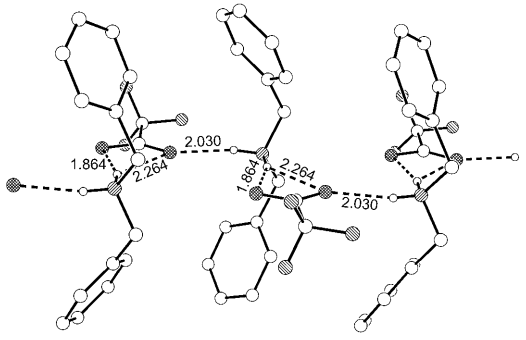

Figure 4. Single crystal X-ray structure of **2**-TFA. Hydrogen bonds are indicated by the dashed lines. The carboxylate oxygen atoms are hydrogen bonded to the N-H protons on the two adjacent cations, forming a noncovalent polymeric structure.

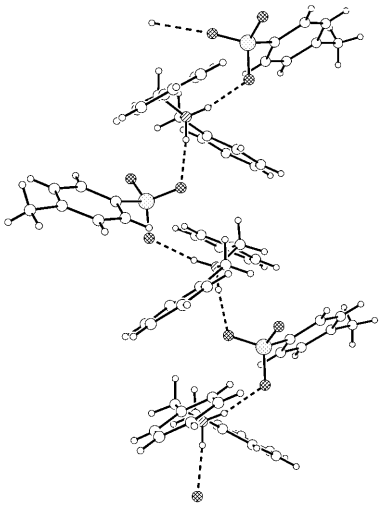

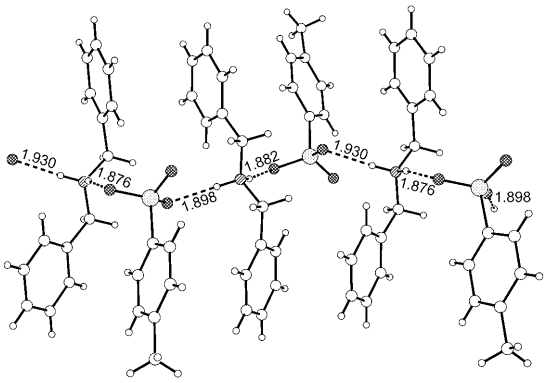

Figure 5. Single crystal X-ray structure of **2**-OTs. Hydrogen bonds are indicated by the dashed lines. The sulfonate oxygen atoms are hydrogen bonded to the N-H protons on the two adjacent cations, forming a noncovalent polymeric structure.

um hexafluorophosphate (TBA-PF_6) was titrated into the solution. As shown in Figure 7, the value of K_{a2} decreased from $3.37\times10^3\,M^{-1}$ at 1.68 mM TBA-PF_6 to a constant value of $2.8\times10^3\,M^{-1}$ above ~15 mM of the TBA salt. Note that this asymptotic limit was quite different from that of Figure 3 ($4.5\times10^2\,M^{-1}$). An asymptotic limit of $K_{a2}=1.6\times10^3\,M^{-1}$ was found when nBu$_4$N$^+$BF$_4^-$(TBA-BF_4) was titrated into a solution of **1** (0.657 mM) and **2**-BF_4 (1.27 mM) (see Supporting Information). Furthermore when an equimolar solution 2.50 mM in both **1** and **2**-TFA reached 50.2 mM in Et$_4$N$^+$ TFA$^-$(TEA TFA) no complex was formed; in this case TEA was found to interact with the crown ether, producing small chemical shifts, attributed to formation of a perching complex (see Supporting Information). The same result was noted with an equimolar solution 1.67 mM in **1** and **2**-OTs upon addition of 50.0 mM TBA-OTs, that is, complexation was essentially prevented.

Interestingly, when the concentration of TBA-PF_6 was held constant at 102 mM, the K_{a2} values were constant ($2.7\times10^3\,M^{-1}$) irrespective of the equimolar concentrations of DB24C8 and **2**-PF_6 (Figure 8), in contrast to the results in Figure 3, but in accord with those of Figure 7.

The report of Montalti and Prodi that addition of TBA-Cl to a solution of **1** and 9-anthrylmethylmethylammonium–PF_6 in CD_2Cl_2 effectively resulted in dethreading of the known pseudorotaxane, a phenomenon attributed to the formation of a tight secondary ammonium chloride ion pair analogous to **2**-Cl,[18] is consistent with the results reported

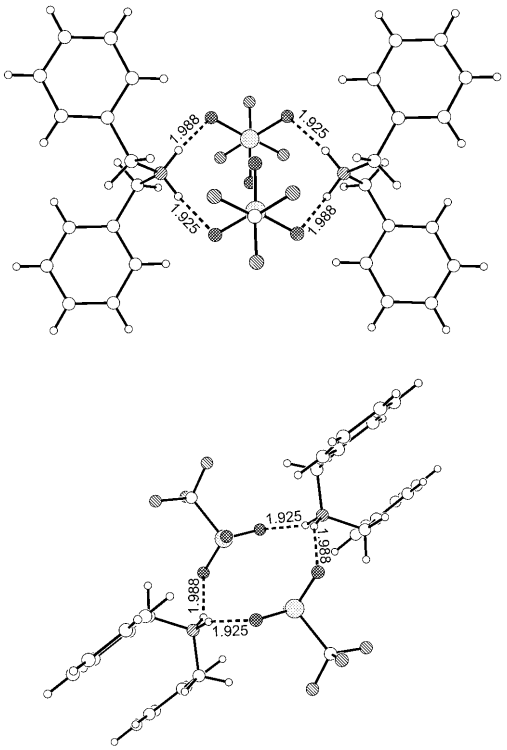

Figure 6. Single crystal X-ray structure of **2**-OTf. Hydrogen bonds are indicated by the dashed lines. The sulfonate oxygen atoms are hydrogen bonded to the N-H protons on the two adjacent cations, forming a noncovalent tetrameric structure.

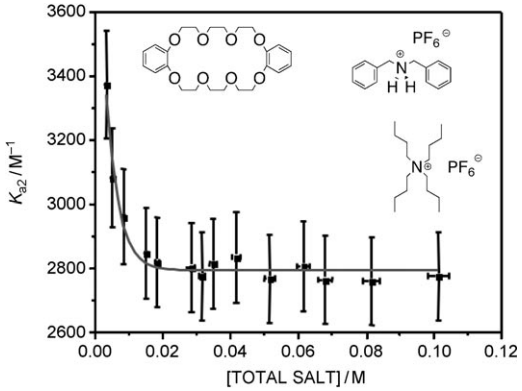

Figure 7. Variation of K_{a2} for DB24C8 and **2**-PF_6 (1.2 mM each in $CD_3CN/CDCl_3$ 2:3, 21.7 °C) in the presence of added TBA-PF_6.

above; for the crystal structure of **2**-Cl, see the Supporting Information. The loss of the complex signal for **1** and **2**-OTs and **1** and **2**-TFA upon the addition of a large excess of $R_4N^+X^-$ (X = OTs or TFA) reflects the fact that quaternary ammonium salts generally dissociate more completely than secondary ammonium salts, because the quaternary cations are more readily solvated than secondary ammonium ions, and the resultant higher concentration of free X^- from the quaternary salt causes increased ion pairing of the dibenzylammonium cation (le Chatelier's principle), resulting in less free $\mathbf{2}^+$ available for complexation. However, the differing

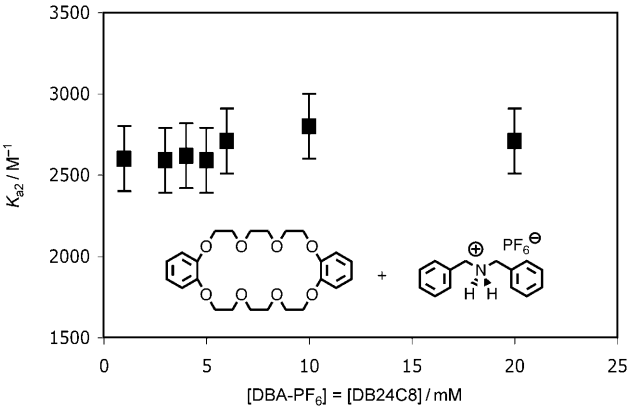

Figure 8. Variation of K_{a2} with equimolar concentration of for DB24C8 and **2**-PF_6 (in $CD_3CN/CDCl_3$ 2:3, 21.7 °C) in the presence of 103 mM TBA-PF_6.

asymptotic limits in Figure 3 and 7 clearly indicate that another factor is involved; in addition to ion pairing, activity coefficients need be considered.

Theory

As shown in Equation (5), we consider ion pair dissociation as a pre-equilibrium step in the complexation process[19] and assume that a) the electrolyte exists in solution as a monomer in equilibrium with its component ions, b) it is the free ammonium ion that forms the complex, the latter being fully dissociated, and c) there are no other species present.

In such systems activity coefficients are an important consideration. The activity coefficient is exponentially related to the inverse 3/2 power of the permittivity; as a result it is extremely sensitive to ionic strength in solvents with low dielectric constants.[20] For example, use of the limiting Debye–Hückel treatment at 298 K in chloroform ($\varepsilon = 4.81$)[21] for salts composed of monovalent ions yields $-\log\gamma_\pm = 33.6\mu^{1/2}$, in which $\gamma_\pm$ is the activity coefficient and μ is the ionic strength. Thus, the activity coefficient of a chloroform solution with an ionic strength of 1.00 mM is estimated to be 0.09 (see Figure 9). Restated, this means that in order for $\gamma_\pm$ to be ≥ 0.90 and simulate ideal bahavior ($\gamma_\pm = 1$) in $CHCl_3$, μ must be less than 1.85×10^{-6} M! Taking the volume average dielectric constant ($\varepsilon = 17.5$) for 3:2 (v:v) $CHCl_3/CH_3CN$, $-\log\gamma_\pm = 4.84\mu^{1/2}$; for an ionic strength of 1.00 mM, $\gamma_\pm = 0.703$. And, for $\gamma_\pm > 0.90$, μ must be less than 8.9×10^{-4} M. With acetonitrile as solvent ($\varepsilon = 38.8$[21]) $-\log\gamma_\pm = 1.47\mu^{1/2}$; for an ionic strength of 1.00 mM, $\gamma_\pm = 0.898$. With acetone as solvent ($\varepsilon = 20.7$[21]) $-\log\gamma_\pm = 3.76\mu^{1/2}$; for an ionic strength of 1.00 mM, $\gamma_\pm = 0.760$. It is clear from these examples that concentration does not approximate activity in these systems, and, therefore, "constants" calculated from concentration-based methods in these low dielectric media are *a priori* questionable.

Inclusion of activity coefficients in Equation (5) yields Equation (5a):

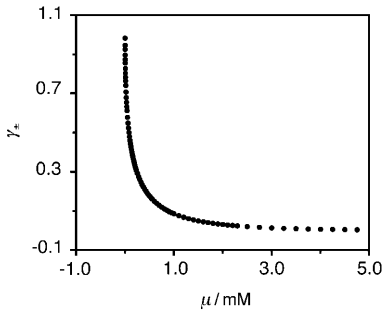

Figure 9. $\gamma_\pm$ vs μ for a monovalent salt, G^+X^-, in $CHCl_3$ at 298 K, as calculated by the limiting Debye–Hückel equation.

$$K_{o5} = \gamma_\pm^2\,[HG^+][X^-]/[H][G^+X^-] \quad (5a)$$

Expressing the overall equilibrium as individual steps in terms of activities:

$$K_{ipd} = \gamma_\pm^2[G^+][X^-]/[G^+X^-] \quad (6)$$

Solving for $[G^+]$:

$$[G^+] = K_{ipd}[G^+X^-]/\gamma_\pm^2[X^-] \quad (6a)$$

and

$$K_{a5} = [HG^+]/[H][G^+] \quad (7)$$

Solving for $[HG^+]$:

$$[HG^+] = K_{a5}\,[H][G^+] \quad (7a)$$

Substituting Equation (6a) into (7a):

$$[HG^+] = K_{a5}\,[H]\,K_{ipd}[G^+X^-]/\gamma_\pm^2\,[X^-] \quad (7b)$$

Conservation of charge requires that

$$[X^-] = [G^+] + [HG^+] \quad (8a)$$

Substitution of Equations (6a) and (7b) into Equation (8a) leads to

$$[X^-] = \{(K_{ipd}[G^+X^-]/\gamma_\pm^2)(1 + K_{a5}[H])\}^{1/2} \quad (8b)$$

Substituting Equation (8b) into Equation (5a):

$$K_{o5} = \gamma_\pm^2\,[HG^+]\{(K_{ipd}[G^+X^-]/\gamma_\pm^2)(1 + K_{a5}[H])\}^{1/2}/$$
$$[H][G^+X^-] = \gamma_\pm[HG^+]\{K_{ipd}(1 + K_{a5}[H])\}^{1/2}/[H][G^+X^-]^{1/2} \quad (5b)$$

Equation (5b) may be evaluated under two extremes. When $K_{a5}[H] \gg 1$ Equation (5b) reduces to

$$K_{o5} = \gamma_\pm[HG^+]\{K_{ipd}K_{a5}[H]\}^{1/2}/[H][G^+X^-]^{1/2}$$
$$= \gamma_\pm[HG^+]\{K_{o5}[H]\}^{1/2}/[H][G^+X^-]^{1/2}$$
$$K_{o5}^{1/2}/\gamma_\pm = [HG^+]/[H]^{1/2}\,[G^+X^-]^{1/2} \quad (5c)$$

Under this condition, that is, when [H] is high, all of the free counterion X^- essentially results from complex formation, and $[HG^+] \approx [X^-]$. Since at infinite dilution $\gamma_\pm = 1$, a plot of the right hand side of Equation (5c) versus $[G^+X^-]_0$ extrapolated to zero concentration will yield K_{o5} as the y intercept. In other words the data are extrapolated to a condition at which the concentrations reflect the activities.

At the other extreme when $K_{a5}[H] \ll 1$ from Equation (5b)

$$K_{o5} = \gamma_\pm[HG^+]K_{ipd}^{1/2}/[H][G^+X^-]^{1/2}$$
$$K_{o5}/\gamma_\pm K_{ipd}^{1/2} = K_{a5}K_{ipd}^{1/2}/\gamma_\pm = [HG^+]/[H][G^+X^-]^{1/2} \quad (5d)$$

Under this condition, that is, when [H] is low, the free counterion is essentially all generated as a result of ion pair dissociation of G^+X^-. A plot of the right hand side of Equation (5d) versus $[G^+X^-]_0$ extrapolated to zero concentration will yield $K_{a5}K_{ipd}^{1/2}$ as the y intercept. Again the data are extrapolated to a condition at which the concentrations reflect the activities, that is, $\gamma_\pm = 1$. Provided both binding regions are experimentally observable, the individual constants may then be determined from the ratio of the intercepts of plots of Equation (5c) and (5d).

Application of the Pre-equilibrium Model

We have applied these treatments to our ^{1}H NMR data for pseudorotaxane **1·2$^+$** formation. Provisionally assuming $K_{a5} = 500\,M^{-1}$, we studied host–guest solutions in which $[\mathbf{1}]_0 \geq 15.0$ mM ($K_{a5}[H] \geq 7.5 \gg 1.0$, error 1/8.5 $\leq$ 12%) and at the other extreme, $K_{a5}[H] \ll 1$, we studied host/guest solutions in which $[\mathbf{1}]_0 \leq 0.500$ mM ($K_{a5}[H] \leq 0.25 \ll 1.0$, error 0.25/1.25 $\leq$ 20%). Plots of Equation (5c) for four counterions are shown in Figure 10. Plots of Equation (5d) are shown in Figure 11. In both plots we used $[G^+X^-] = [G^+X^-]_o - [HG^+]$; see Supporting Information for a discussion of the errors introduced by this approximation, which decrease in the order $PF_6 > BF_4 > OTs > TFA$ and approach zero at low salt concentration.

It is interesting to compare the intercepts of these plots. From Figure 10 the values of $K_{o5}^{1/2}$ are 1.88, 1.40, 0.489 and 0.304, respectively, for $X = PF_6$, BF_4, OTs and TFA. Note that $K_{o5}^{1/2} = [K_{ipd}K_{a5}]^{0.5}$. Since K_{a5} is identical for all of the counterions, the intercepts yield the following ratios: $K_{ipd\,PF_6}/K_{ipd\,BF_4} = 1.80$, $K_{ipd\,PF_6}/K_{ipd\,OTs} = 14.7$, $K_{ipd\,PF_6}/K_{ipd\,TFA} = 38.2$. From Figure 11 the values of $K_{a5}\,K_{ipd}^{1/2}$ are 42.4, 31.3, 10.9 and 6.76, respectively, for $X = PF_6$, BF_4, OTs and TFA. From the values from these plots we can calculate the following

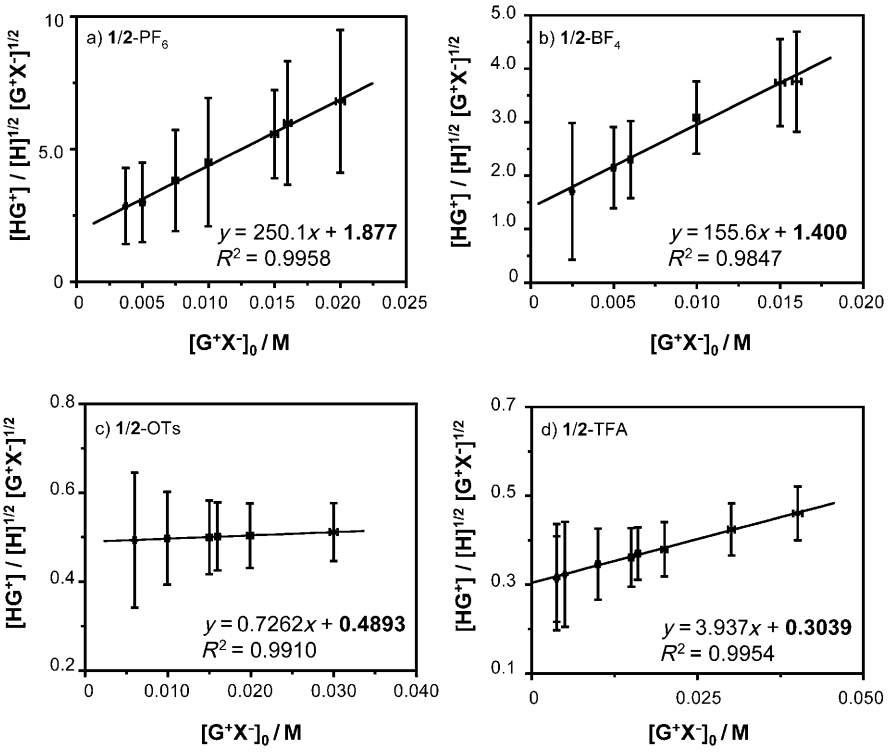

Figure 10. Plots of Equation (5c) ($K_{a5}[H] \gg 1$) for solutions of **1** and a) **2**-PF_6, b) **2**-BF_4, c) **2**-OTs, and d) **2**-TFA in $CDCl_3/CD_3CN$ 3:2, 295 K.

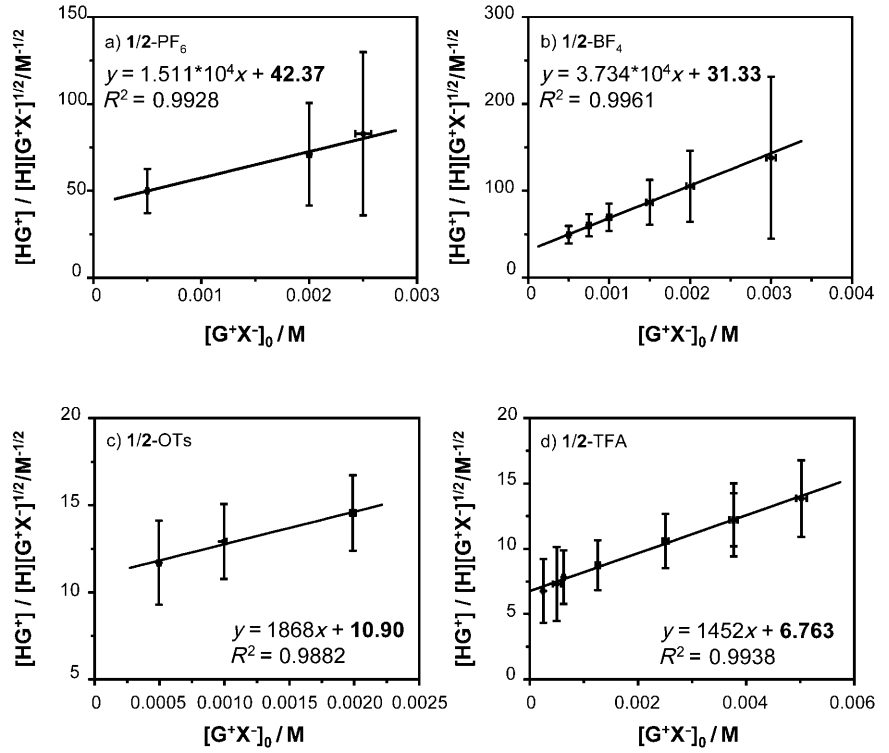

Figure 11. Plots of Equation (5d) ($K_{a5}[H] \ll 1$) for solutions of **1** and a) **2**-PF_6, b) **2**-BF_4, c) **2**-OTs, and d) **2**-TFA in $CDCl_3/CD_3CN$ 3:2, 295 K.

ratios: $K_{ipdPF_6}/K_{ipdBF_4} = 1.83$, $K_{ipdPF_6}/K_{ipdOTs} = 15.1$, $K_{ipdPF_6}/K_{ipdTFA} = 39.2$. The latter values from Equation (5d) are in excellent agreement (±3% relative) with the values calculated using Equation (5c); this self-consistency provides corroboration of the validity of the approach, since the two sets of measurements are basically independent of each other. Table 1 summarizes the individual constants.

The values of K_{ipd} in Table 1 are roughly in accord with reported activity-based values for tetraalkylammonium salts[22] and concur with the observation that PF_6 salts are generally the most dissociated.[23] To appreciate the effect of the differences in K_{ipd}, consider the following extents of ionization calculated for solutions of the DBA salts alone at 1.00 (10.0) mM: PF_6: 90% (55%); BF_4: 82% (46%); OTs: 49% (19%); TFA: 35% (12%). Moreover, the values of K_{a5} for all the salts are identical within experimental error, as mandated by this equilibrium treatment. Because Table 1 includes analysis based on activity coefficients, whereas all other previously published values assume $\gamma_{\pm} = 1$, we believe these to be the most accurate K_{a5} values reported to date for pseudorotaxane **1·2**$^+$ formation.

With K_{a5} and K_{ipd} in hand, $\gamma_{\pm}$ may be calculated for each data point according to Equations (5c) and (5d). Figure 12 displays these results for all **1** and **2**-X solutions and demonstrates the large variation in experimental $\gamma_{\pm}$ with $[G^+X^-]_0$. The existence of two families of activity curves is not unexpected: when $K_{a5}[H] \gg 1$ (Figure 12, top dotted curves), complex cations **1·2**$^+$ dominate; at the other extreme (Figure 12, $K_{a5}[H] \ll 1$, bottom solid curves), guest cations **2**$^+$ domi-

Table 1. Equilibrium constants for **2**-X salts with **1** calculated from Equation (5c) and (**5d**) [$CDCl_3/CD_3CN$ 3:2, 295 K].

X	Intercept (A) of Figure 10 Equation (5c)	Intercept (B) of Figure 11, Equation (5d)	$K_{os}=A^2$	K_{as} [M^{-1}][a]	K_{ipd} [M][b]
PF_6	1.88 ± 0.08	42.4 ± 1.4	3.53 ± 0.33	509 ± 80	$6.94\ (\pm3.40)\times10^{-3}$
BF_4	1.40 ± 0.10	31.3 ± 1.0	1.96 ± 0.28	500 ± 110	$3.92\ (\pm3.00)\times10^{-3}$
OTs	0.489 ± 0.001	10.9 ± 0.3	0.239 ± 0.001	497 ± 30	$4.80\ (\pm0.80)\times10^{-4}$
TFA	0.304 ± 0.002	6.76 ± 0.11	0.0924 ± 0.0012	495 ± 30	$1.85\ (\pm0.30)\times10^{-4}$
ave	–	–		500 ± 63	–

[a] $K_{as}=(B/A)^2$. [b] $K_{ipd}=(B/K_{as})^2$.

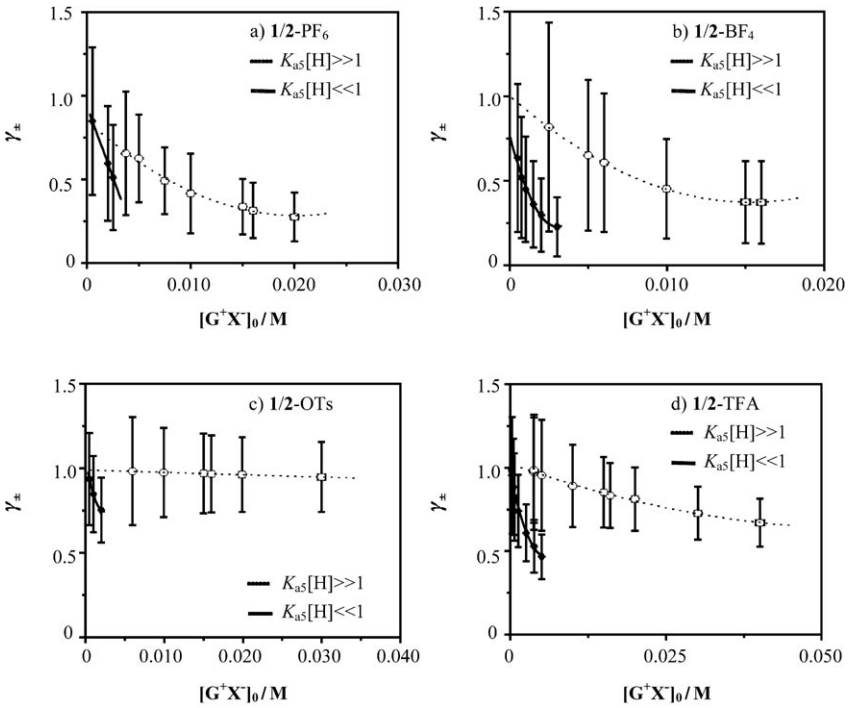

Figure 12. $\gamma_{\pm}$ as calculated according to Equation (5c) ($K_{as}[H]\gg1$, top dotted curves) and Equation (5d) ($K_{as}[H]\ll1$, bottom solid curves) vs. $[G^+X^-]_0$ for solutions of **1** and a) **2**-PF_6, b) **2**-BF_4, c) **2**-OTs, and d) **2**-TFA in $CDCl_3/CD_3CN$ 3:2, 295 K. The lines have been added to guide the eye.

nate. Interestingly, in the $K_{as}[H]\gg1$ regime, $\gamma_{\pm}$ changes less than is the case when $K_{as}[H]\ll1$. This is most likely a consequence of the lower solvation energy of the larger pseudorotaxane cation **1·2**$^+$ relative to **2**$^+$, as described to a first approximation by the Born model.[24] We speculate that this is due to delocalization of charge in the pseudorotaxane cation, which would effectively impart more "ideal" character to the complex ion, **1·2**$^+$, than is the case for the "naked" 2° ammonium ion, **2**$^+$.

The activity coefficients vary significantly with the anion. The logarithms of the activity coefficients are linear with the salt concentrations as described in Figures 13 and 14 for the two extreme cases; this is in accord with Debye–Hückel theory.

It is interesting to compare the effects of different anions on the activity coefficients. As seen in Table 2 there is a wide variation both when $K_{as}[H]\ll1$ and when $K_{as}[H]\gg1$. Under most conditions the tosylate salt behaves nearly ideally, that is, $\gamma_{\pm}\sim1$. The decrease in activity coefficient follows the order OTs > TFA > PF_6 > BF_4 for $K_{as}[H]\ll1$ and OTs > TFA > BF_4 ≥ PF_6 for $K_{as}[H]\gg1$. Note the fact that BF_4 and PF_6 switch positions in the two different regimes.

Looking back to Figures 3, 7 and 8, we can now rationalize the results. In Figure 3 in the plateau region $K_{as}[\mathbf{1}]\gg1$. In Figure 7 $K_{as}[\mathbf{1}]<1$ and ions from TBA-PF_6 predominate; in this case the pseudorotaxane cation and the dibenzylammonium cation are at relatively low concentrations. The results shown in Figure 8 indicate that even when the concentrations of the host and guest are increased the effect of the added quaternary salt is dominant and thus the ultimate value of K_{a2} is the same in Figures 7 and 8. The plateau in Figure 3 corresponds to the situation in which the value of $K_{os}/\gamma_{\pm}^2\,[X^-]$ is constant, meaning that the product $\gamma_{\pm}^2\,[X^-]$ is constant; in other words, in this regime the increasing anion concentration is offset by the change in activity coefficient. The reasons that the plateau values of Figures 3, 7 and 8 are different are twofold: 1) because of the higher K_{ipd} value for TBA-PF_6 relative to **2**-PF_6 the ionic strength is higher in the latter cases, causing a smaller $\gamma_{\pm}$ and, 2) in the latter two cases (Figures 7 and 8) the presence of the tetrabutylammonium cation likely alters the average value of $\gamma_{\pm}$.

Direct Determination of K_{ipd} Values

In our early work, we attributed changes in the chemical shifts of the uncomplexed dibenzylammonium species, particularly the benzylic protons, to time-averaged *exo* or perching type complexation with the crown ether;[12a] however, it now clear that the major cause of these chemical shift changes is time averaging caused by the dynamic ion pair equilibrium of the salt as it responds to the free X^- generated by formation of the pseudorotaxane complex. Other authors have used chemical shift data to estimate K_{ipd} values for various salts in organic solvents;[25] however, they ignor-

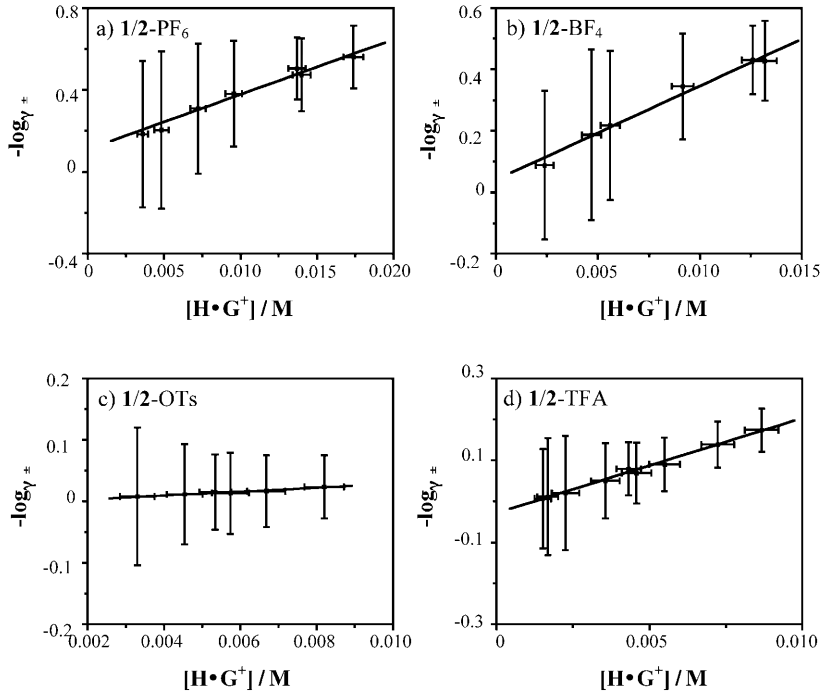

Figure 13. Plots of $-\log\gamma_{\pm}$ versus [**1**·**2**$^+$] for solutions of **1** and a) **2**-PF_6, b) **2**-BF_4, c) **2**-OTs, and d) **2**-TFA in $CDCl_3/CD_3CN$ 3:2, 295 K, $K_{a5}[H] \gg 1$.

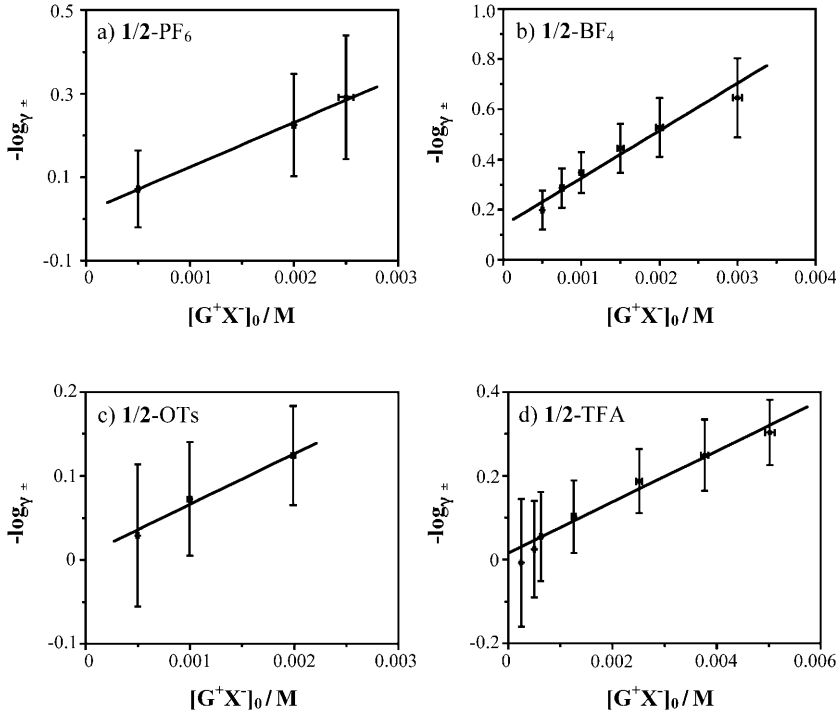

Figure 14. Plots of $-\log\gamma_{\pm}$ versus $[\mathbf{2}\text{-X}]_0$ for solutions of **1** and a) **2**-PF_6, b) **2**-BF_4, c) **2**-OTs, and d) **2**-TFA in $CDCl_3/CD_3CN$ 3:2, 295 K, $K_{a5}[H] \ll 1$.

ed changes in activity coefficients, which will affect different points along the curve differently. In principle the same approach described above could be employed, except that the ion pairing equilibria are fast exchange and thus one must determine the chemical shifts of the free cation and the fully ion-paired cation. We examined a number of the salts **2**-X as functions of their concentrations; all displayed concentration dependent chemical shifts, particularly for the benzylic protons. For **2**-PF_6 and **2**-TFA we observed anomalous behavior in terms of chemical shifts at both very high and very low concentrations (see Supporting Information), thus making estimation of the chemical shifts of the free and fully ion paired cation precarious. In view of the possibility of formation of more complicated species, such as triple ions,[25e,26] at the extremes, we consider estimation of K_{ipd} values for these salts using ^{1}H NMR data to be questionable.

Utilization of the Model as a Predictive Tool

Due to the fact that the activity coefficients vary significantly with concentration, prediction of extents of complexation using the derived K_{ipd} and K_{a5} values becomes a daunting task. To illustrate, in Figure 15 $[H{\cdot}G^+]/[G^+X^-]^{1/2}$ (determined experimentally) is plotted versus $[H{\cdot}G^+]/[G^+X^-]^{1/2}$ calculated according to rearranged Equation (5b) assuming $\gamma_{\pm}=1$, $K_{a5}=5.1\times10^2\,\text{M}^{-1}$ and $K_{ipd}=6.9\times10^{-3}\,\text{M}$; the line corresponds to a perfect relationship. There is a clear lack of agreement between predicted and experimental values. These results reflect the fact that the activity coefficient is lower at higher ionic strength, leading to relatively greater extents of complexation on a molar basis relative to the low ionic strength situation, as can be seen from Equation (7b). These results also reflect the dependence of the activity coefficient on the nature of the predominant cation, whether the free *sec*-ammonium cation (**2**$^+$) or the pseudorotaxane complex

Table 2. Variation of experimental activity coefficients ($\gamma_{\pm}$) with concentration and anion in $CDCl_3/CD_3CN$ 3:2.

		$K_{a5}[H] \ll 1$			$K_{a5}[H] \gg 1$	
[**1**]/[**2**-X]/mM mM →	0.50/0.50	0.50/1.00	0.50/2.00	20.0/15.0	20.0/10.0	16.0/16.0
X = OTs	0.93	0.84	0.75	0.98	0.99	0.98
X = TFA	0.91	–		0.84	0.87	0.82
$X = BF_4$	0.85	0.44	0.29	0.38	0.45	0.38
$X = PF_6$	0.62	–	0.60	0.34	0.42	0.32

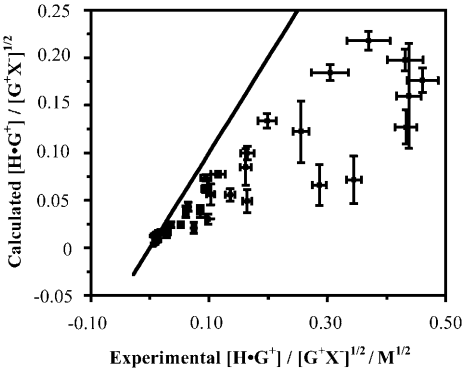

Figure 15. Plot of $[H{\cdot}G^+]/[G^+X^-]^{1/2}$ calculated according to Equation (5b) (solid line, $\gamma_{\pm}=1$) versus $[H{\cdot}G^+]/[G^+X^-]^{1/2}$ determined experimentally for solutions of **1** and **2**-PF_6, in $CDCl_3/CD_3CN$ 3:2, 295 K.

(**1**·**2**$^+$). Disregard of $\gamma_{\pm}$ in estimation of equilibrium constants amounts to the assumption that $\gamma_{\pm}=1$ and mirrors the widespread use of invalid Equation (2) [or Eq. (3)] in the literature.

To utilize the binding constants for their intended purpose as predictive tools, activity coefficients must therefore be known (or be capable of being estimated) a priori. While the activity coefficients are well-behaved in each binding regime (Figures 13 and 14), they are dependent on the nature of the anion and the concentrations. Based on these considerations, we conclude that it is difficult, if not impossible, to use the two equilibrium constants involved in these processes to predict extents of complexation.

Comparisons between Hosts for Any Given Guest

On a more positive note, however, results from these studies suggest an experimental method to compare the binding efficiencies of two or more hosts for any given guest in a precise manner. Such a comparison is of great practical interest: the ultimate goal in many host/guest studies is the development of a host moiety that selectively and strongly binds a specific guest species; for example, the formation of high molecular weight supramolecular polymers from small molecule building blocks requires very high association constants ($>10^4\,M^{-1}$).[27] As shown in Figures 7 and 8 the extent of complexation approaches an asymptotic limit upon addition of a salt whose cation does not interact with the host and whose anion is identical to that of the guest. The addition of a large excess of salt (N^+X^-) such that essentially all of the free anion results from ion pair dissociation of this salt alone ($K_{ipd,NX}$) affords a quantitative means of evaluating relative cation binding constants, K_{a5}, as follows:

$$K_{ipd,NX} = \gamma_{\pm}^{\,2}\,[N^+][X^-]/[N^+X^-] \quad (9)$$

Solving for $[X^-]$:

$$[X^-] = \{K_{ipd,NX}\,[N^+X^-]/\gamma_{\pm}^{\,2}\}^{1/2} \quad (9a)$$

Substitution of Equation (9a) into Equation (5a) leads to

$$K_{o5} = K_{ipd,\mathbf{2}\text{-}X}K_{a5} = \gamma_{\pm}[HG^+]\,\{K_{ipd,NX}\,[N^+X^-]\}^{1/2}/[H][G^+X^-] \quad (10)$$

$$K_{a5} = (\gamma_{\pm}\{K_{ipd,NX}\,[N^+X^-]\}^{1/2}/K_{ipd,\mathbf{2}\text{-}X})\,[HG^+]/[H][G^+X^-] = (\text{constant})\,[HG^+]/[H][G^+X^-] \quad (10a)$$

Equation (10a) provides a means of evaluating the relative values of K_{a5} for two or more hosts and any given guest in the presence of excess N^+X^-. Thus, from Equation (10a) the ratio $K_{a5,A}/K_{a5,B}$ is equivalent to the ratio $([H_AG^+]/[H_A][G^+X^-])/([H_BG^+]/[H_B][G^+X^-])$, providing a rigorous quantitative comparison of binding efficiencies of the two hosts A and B. In fact we have applied this method in two published cases. We showed that the dibenzylammonium pseudorotaxane complexes of the *syn*- and *anti*-isomers of bis(carbomethoxy)dibenzo-[30]crown-10 were not ion-paired in $CDCl_3/CD_3CN$ 3:2, thereby displaying the same concentration dependent K_{a2} behavior described here; however, application of the above treatment allowed us to determine the K_{a5} value for these two hosts based on the now known K_{a5} for DB24C8 (**1**) under the same conditions.[13f] Likewise K_{a5} for a polystyryl DB24C8 with the dibenzylammonium cation was also determined.[28]

Final Comments

It should be noted that the more soluble the salt in low polarity organic solvents, the greater the ionization constant, K_{ipd}, and consequently the higher the ionic strength and thus the lower the activity coefficient. This can be seen by inspection of Table 2; the more soluble BF_4 and PF_6 salts display lower activity coefficients relative to the less soluble OTs and TFA salts. Therefore, the choice of the more soluble salts actually complicates the analysis, while at the same time it increases the extent of complexation as a result of a

higher cation concentration and the lower activity coefficient [see Eq. (5e)].

$$[HG^+] = K_{os}[H][G^+X^-]/\gamma_{\pm}{}^2[X^-] \quad (5e)$$

Conclusion

These studies reveal the importance of correctly defining equilibria when deriving quantitative descriptions of host–guest interactions. When salts are involved, particularly in low dielectric constant solvents, ion pairing must be considered. This may be easily done by comparing K_{a2} or K_{a3} values for a given system at various starting component concentrations. If K_{a2} or K_{a3} values do not vary with [host] or [guest], then either the salt and the complex are both ion-paired [Eq. (2)] or the salt and the complex are both essentially not ion paired [Eq. 3)]. In these circumstances, provided activities may be estimated in the second case, a single point determination of K_a at any given temperature may be adequate.

On the other hand, if K_{a2} or K_{a3} values fluctuate with concentration, it indicates that the situation described by Equation (5) obtains and a broad range of host and guest concentrations must be examined to properly quantify binding. Moreover, because activity varies with temperature, extensive studies would have to be run at all temperatures to derive meaningful thermodynamic parameters ΔH^0 and ΔS^0. Failure to consider the low activity coefficients of salts at NMR concentrations (>1 mM) in low dielectric media can lead to erroneous analyses of such systems. For example, it may lead to use of curve fitting-based ("black-box") routines that employ undetected or hypothesized species to account for the resultant deviations from simpler theories. Note that use of UV/Vis or fluorescence[29] spectroscopic measurements allows lower concentrations to be employed, relative to NMR, and salts may be completely ionized or nearly so and the situation is described by Equation (3) with appropriate account of activity coefficients; however, the results from such measurements cannot be extended to higher concentrations without due consideration of the issues raised here. Similar reservations apply to use of titration microcalorimetry to study such systems; great care must be taken, since normally the software does not take account of situations described by Equation (5).[8j] Unfortunately even a rigorous analysis suffers the same end result; the resultant association constants cannot predict concentrations of all species at all concentrations, because the activity coefficients cannot be predicted with confidence. These findings are in accord with a former colleague's [Charles B. ("Charlie") Duke] conclusions that: "…1) All theories are wrong; it's just a matter of degree. 2) All experiments measure something. It's probably not what you think they measure, and if it is, not to the precision needed."…[30]

However, this research did result in the development of a method to determine the relative binding constants for various hosts with a given guest by the addition of a tetrabutylammonium salt with the same anion (X^-) as the guest salt (**2**-X).

Furthermore, as we observed earlier, complexation of the counterion X^- in these situations will lead to a higher percentage of complexation of the cations because the dissociation to the free cations will be encouraged (le Chatelier's principle).[11] Indeed this realization has resulted in the synthesis of ditopic hosts capable of binding both the anionic and cationic species with greater affinity.[31]

Experimental Section

General experimental procedures: Dibenzo-[24]crown-8 (**1**) was purchased commercially and used without further purification. All solvents were used as received from the vendor. Melting points were determined in a Mel-temp II melting point apparatus and are corrected. All proton NMR spectra were recorded on Varian Unity or Inova 400 MHz instruments using tetramethylsilane as an internal standard; the following abbreviations are used: b (broad), s (singlet), d (doublet), m (multiplet), t (triplet), ArH (aromatic hydrogen). Elemental analyses were performed by Atlantic Microlab, Inc., Norcoss, GA.

Dibenzylammonium chloride (2-Cl): A described by Stoddart et al.[13c] a 12.2 M stock HCl solution (42 mL) was transferred to a 250 mL round-bottom flask and diluted with dionized water to yield a 2.0 M HCl solution. To this solution, dibenzylamine (4.9416 g, 25.05 mmol) was slowly added, whereupon the white precipitate of dibenzylammonium chloride was immediately observed. The mixture was allowed to stir for 6 h before the chloride salt was collected via vacuum filtration, recrystallized from H_2O (3×) and dried (4.60 g, 80%). M.p. 275–277 °C (lit., not reported); ^{1}H NMR (DMSO, 400 MHz): δ = 9.89 (br s, 2H), 7.57 (d, J=7 Hz, 4H), 7.43–7.37 (m, 6H), 4.10 ppm (s, 4H); elemental analysis calcd (%) for $C_{14}H_{16}NCl$: C 71.94, H 6.90, N 5.99; found: C 71.91, H 6.83, N 5.96.

Dibenzylammonium hexafluorophosphate (2-PF$_6$): Also described by Stoddart et al.,[13c] warm, deionized water (100 mL) was added to dibenzylammonium chloride (4.6 g, 20 mmol). Heating resulted in complete solvation of the chloride salt, whereupon slow addition of saturated aqueous ammonium hexafluorophosphate yielded a thick, white precipitate that was collected via vacuum filtration, washed excessively with warm water and dried (4.30 g, 64%). M.p. 208–210 °C (lit.: 192–193 °C,[13c] 207–209 °C[32]); ^{1}H NMR (CD_3CN, 400 MHz): δ = 7.49 (s, 10H), 4.25 ppm (s, 4H); elemental analysis calcd (%) for $C_{14}H_{16}NPF_6$: C 48.99, H 4.70, N 4.08; found: C 48.97, H 4.62, N 3.99.

Dibenzylammonium methanesulfonate (2-OMs): Methanesulfonic acid (1.00019 g, 10.41 mmol) was added to diethyl ether (100 mL) at room temperature and dibenzylamine (2.00 mL, 10.4 mmol, via a 2 mL TD volumetric pipette) were added dropwise to the stirred acid solution, resulting in an immediate white precipitate. The precipitate was collected via vacuum filtration, washed with copious amounts of diethyl ether, and dried (3.05 g, 95%). M.p. 135–137 °C (lit., not reported); ^{1}H NMR ($CDCl_3$, 400 MHz): δ = 9.24 (br s, 2H), 7.45 (d, J=8 Hz, 4H), 7.39–7.30 (m, 6H), 3.94 (t, J=5 Hz, 4H), 2.60 ppm (s, 3H); elemental analysis calcd (%) for $C_{15}H_{19}NO_3S$: C 61.41, H 6.53, N 4.77; found: C 61.21, H 6.49, N 4.70.

Dibenzylammonium *p*-toluenesulfonate (2-OTs): *p*-Toluenesulfonic acid (2.8533 g, 15.13 mmol) was dissolved in methanol (25 mL) at room temperature. Dibenzylamine (2.9660 g, 15.03 mmol) was added dropwise to the stirred acid solution, resulting in a white precipitate. The precipitate was collected via vacuum filtration, washed with cold methanol, and dried (5.35 g, 92%). M.p. 166–168 °C (lit., not reported); ^{1}H NMR ($CDCl_3$, 400 MHz): δ = 9.27 (br s, 2H), 7.59 (d, J=8 Hz, 2H), 7.38 (m, 4H), 7.27 (m, 6H), 7.13 (d, J=8 Hz, 2H), 3.91 (t, J=5 Hz, 4H), 2.38 ppm (s, 3H); elemental analysis calcd (%) for $C_{21}H_{23}NO_3S$: C 68.27, H 6.27, N 3.79; found: C 68.09, H 6.23, N 3.80.

Dibenzylammonium tetrafluoroborate (2-BF_4): Tetrafluoroboric acid, 54% by weight in diethyl ether (1.55 g, 18 mmol), was added to diethyl ether (100 mL) at room temperature. Dibenzylamine (2.00 mL, 10.4 mmol, via a 2 mL TD volumetric pipette) was added dropwise to the stirred acid solution. A white precipitate was observed immediately, collected via vacuum filtration, washed with diethyl ether and dried (2.00 g, 68%). M.p. 196–198°C (lit. 186°C[33]); ^{1}H NMR ($CDCl_3$, 400 MHz): δ = 7.37 (s, 10H), 4.03 ppm (s, 4H); elemental analysis calcd (%) for $C_{14}H_{16}NBF_4$: C 58.98, H 5.66, N 4.91; found: C 59.10; H 5.61; N 4.97.

Dibenzylammonium trifluoromethanesulfonate (2-OTf): Trifluoromethanesulfonic acid (1.64494 g, 10.96 mmol) was added to diethyl ether (~100 mL) at room temperature. Dibenzylamine (2.00 mL, 10.40 mmol, via a 2 mL TD volumetric pipette) was added dropwise to the stirred acid solution. A white precipitate was observed and collected via vacuum filtration, washed with diethyl ether and dried (2.60 g, 72%). M.p. 115–117°C (lit., no report); ^{1}H NMR ($CDCl_3$, 400 MHz): δ = 8.18 (brs, 2H), 7.39 (m, 10H), 3.97 ppm (t, J=5 Hz, 4H); elemental analysis calcd (%) for $C_{15}H_{16}NF_3SO_3$: C 51.87, H 4.84, N 4.03; found: C 51.90, H 4.64, N 3.99.

Dibenzylammonium trifluoroacetate (2-TFA): Trifluoroacetic acid (15.4 mL, 200 mmol) was added to a 100 mL volumetric flask and diluted with dionized water, to yield a 2.00 M solution. Dibenzylamine (1.98254 g, 10.24 mmol) was added to a round bottom flask, to which the TFA solution was slowly added. A white precipitate was immediately observed and collected via vacuum filtration, washed with water, and dried (2.23 g, 71%). M.p. 147–149°C (lit. no report); ^{1}H NMR ($CDCl_3$, 400 MHz): δ = 9.90 (brs, 2H), 7.21–7.31 (m, 10H), 3.81 ppm (t, J=5 Hz, 4H); elemental analysis calcd (%) for $C_{16}H_{16}NO_2F_3$: C 61.73, H 5.18, N 4.50; found: C 61.63, H 5.28, N 4.42.

Crystallography: Long thin needles (~$1.0\times0.2\times0.01$ mm^3) of **2**-OTs, **2**-TFA, and **2**-OTf were crystallized by vapor diffusion of pentane into chloroform solution at room temperature. A needle was cut (~$0.2\times0.1\times0.02$ mm^3), mounted on a nylon CryoLoop (Hampton Research) with Krytox Oil (DuPont) and centered on the goniometer of a Oxford Diffraction XCalibur2 diffractometer equipped with a Sapphire 2CCD detector. The data collection routine, unit cell refinement, and data processing were all carried out with the program CrysAlis.[34] The Laue symmetry and systematic absences were consistent with the monoclinic space groups $P2_1/n$. The structure was solved by direct methods and refined using the SHELXTL 97 program package.[35] The final refinement involved an anisotropic model for all non-hydrogen atoms. Hydrogen atom positions and isotropic thermal parameters were refined independently.

Preparation of solutions and ^{1}H NMR analyses: To minimize experimental error in these studies, solutions were prepared by precisely weighing a minimum of 1.0×10^{-2} ($\pm5\times10^{-5}$) g each host and guest component by means of an analytical balance which read to 1.0×10^{-4} g into a 5.00 ($\pm$0.02) or 10.00 ($\pm$0.02) mL volumetric flask equipped with a ground glass stopper to make a moderately concentrated (nominally 16.0 mM) master solution. A $CD_3CN/CDCl_3$ 2:3 (by volume) solvent mixture was chosen because the **2**-X salts investigated displayed a wide range of solubility behaviors in the lower dielectric constant solvent, whereas they were all well-solvated by CH_3CN. This solution was then sequentially diluted (no more than four sequential dilutions per master solution) by transferring specific volumes of the higher concentration solution to a clean volumetric flask via a to-deliver volumetric pipette ($\pm$0.006 mL) and diluting to the mark. The fresh solutions were filtered through a cotton-filled disposable pipette before 0.500 ($\pm$0.006) mL of each solution component (both host and guest) at a specified concentration was transferred via a to-deliver pipette to a 5.0 mm NMR tube. NMR spectroscopic data were collected on a temperature controlled 400 MHz spectrometer within 1 hour of mixing the solutions. Table 3 displays results for the full data sets utilized in these studies. When $K_{ap}[H] \gg 1$, the fraction of total crown moieties occupied by guest was determined by integration of the complexed and uncomplexed crown signals H_γ and/or $H_{ar,H}$; the same signals were followed when $K_{ap}[H] \ll 1$ and $[H]_0 \geq [G^+X^-]_0$. When $K_{ap}[H] \ll 1$, and $[H]_0 < [G^+X^-]_0$, the fraction of host occupied (represented by θ) was determined by integration of the complexed and uncomplexed guest signals H_1 and/or $H_{ar,G}$.

Maximum possible concentration errors were calculated by accumulation (summing) of weighing and dilution errors. For example, the error in preparing [**1**] = 0.985 mM was calculated as follows: 1.1104×10^{-2} g of **1** (error in weighing = 5.0×10^{-5} g/0.01104 g = 0.45%) was added to a 5.00 mL volumetric flask and diluted to the mark (dilution error = 2.0×10^{-5} L/

Table 3. Fraction of crown ether complexed (θ) as a function of $[\mathbf{1}]_0$ and $[\mathbf{2}\text{-X}]_0$, $CDCl_3/CD_3CN$ (3:2), 22°C.

$[\mathbf{1}]_0$ [mM]	$[\mathbf{2}\text{-PF}_6]_0$ [mM]	θ	$[\mathbf{1}]_0$ [mM]	$[\mathbf{2}\text{-BF}_4]_0$ [mM]	θ	$[\mathbf{1}]_0$ [mM]	$[\mathbf{2}\text{-OTs}]_0$ [mM]	θ	$[\mathbf{1}]_0$ [mM]	$[\mathbf{2}\text{-TFA}]_0$ [mM]	θ
20.0	4.99	0.241	20.0	15.0	0.659	20.0	30.0	0.410	20.0	20.0	0.275
20.0	20.0	0.872	20.0	10.0	0.458	20.0	19.9	0.334	16.0	16.0	0.271
20.0	15.0	0.698	20.0	6.01	0.28	20.0	15.0	0.287	16.0	16.0	0.290
20.0	9.99	0.478	20.0	4.99	0.234	20.0	9.93	0.227	8.00	8.00	0.269
20.0	7.50	0.361	20.0	2.49	0.119	16.0	16.0	0.350	8.00	8.00	0.258
20.0	4.99	0.241	16.0	16.0	0.790	8.00	8.00	0.336	4.00	4.00	0.224
14.9	3.73	0.241	8.00	8.00	0.759	8.00	8.00	0.329	4.00	4.00	0.241
10.0	3.73	0.343	8.00	8.00	0.761	4.00	4.00	0.325	3.82	20.0	0.501
7.45	3.73	0.446	4.00	4.00	0.707	4.00	4.00	0.304	3.82	15.4	0.442
5.00	3.73	0.636	4.00	4.00	0.709	3.82	3.75	0.306	3.82	10.0	0.373
4.00	4.00	0.716	3.82	3.74	0.688	2.00	2.00	0.294	3.82	7.71	0.324
3.73	3.80	0.646	3.73	3.81	0.679	2.00	2.00	0.279	3.82	5.00	0.272
3.73	3.73	0.771	3.72	3.83	0.723	1.89	3.75	0.365	3.82	3.85	0.237
3.73	1.93	0.437	2.00	2.00	0.620	1.20	3.75	0.418	3.82	3.77	0.269
3.73	1.19	0.285	2.00	2.00	0.662	1.00	1.00	0.240	3.82	3.76	0.232
3.73	0.918	0.231	1.00	1.00	0.562	1.00	1.00	0.241	2.00	2.00	0.207
3.73	5.00	0.85	1.00	1.00	0.565	0.95	3.75	0.444	2.00	2.00	0.225
2.00	2.00	0.668	0.492	2.00	0.8	0.492	1.99	0.382	1.20	3.77	0.408
1.89	3.73	0.710	0.492	1.50	0.728	0.492	0.997	0.275	1.00	1.00	0.219
1.00	1.00	0.588	0.492	1.00	0.663				0.75	3.77	0.405
1.00	0.998	0.575	0.492	0.751	0.567				0.502	5.02	0.489
0.492	3.75	0.802	0.492	0.500	0.443				0.502	2.51	0.339
0.492	2.50	0.792							0.502	1.26	0.236
0.492	2.00	0.742							0.34	3.77	0.424
0.492	0.999	0.672									
0.492	0.500	0.454									

5.00×10^{-3} L = 0.4%). 2.00 mL of this 4.92 mM solution of **1** was then transferred by means of a volumetric pipette (pipette error = 6.0×10^{-6} mL/2.00×10^{-3} mL = 0.3%) to a 10 mL volumetric flask and diluted to the mark (dilution error = 2.0×10^{-5} L/10.00×10^{-3} L = 0.2%) to yield [**1**] = 0.985 mM. The cumulative error is thus 1.35%, while the random error (the square root of the sum of the squares of the individual errors) is 0.70%. When equal volumes of host and guest of the same concentration are mixed, for this step the cumulative error in both components is 1.2% (6.0×10^{-6} mL/5.0×10^{-3} L), while the random error is 0.63%.

Spectrometer-based errors were determined by preparing seven independent master solutions 8.00 mM in **1** and seven independent master solutions 8.00 mM in **2**-TFA. A total of twelve independent **1**/**2**-TFA mixtures at 4.00 mM in each component were then investigated by following H_γ, chosen because the pseudorotaxane resonance is well resolved from that of the free host. The average percentage of complexed crown was 23.9%, with a standard deviation of 0.3% (Table 4). Nearly identical percent binding and standard deviations were found for the aromatic (24.2%, ±0.3%) and benzylic (23.5%, ±0.4%) protons of **2**-TFA. Because integration limits were manually set in these studies, and thus error introduced, a randomly chosen sample from the above twelve **1**/**2**-TFA mixtures was further examined. Five independent Fourier transformations yielded a standard deviation in percent binding of 0.1%, signifying the high reproducibility of manual transformations (Table 5). Of note, these studies were performed over the course of a full year: although relative humidity fluctuated greatly over this time frame, percent complexation did not. We conclude that atmospheric water has little influence on binding properties of samples prepared and exmined in this manner.

Table 4. Fraction of host occupied by guest (θ) for twelve independently prepared solutions initially 4.00 mM in both **1** and **2**-TFA, $CDCl_3/CD_3CN$ (3:2), 295 K.

Trial	$\theta^{[a]}$	$\theta^{[b]}$	$\theta^{[c]}$	$\theta^{[d]}$
1	0.240	0.250	0.238	0.230
2	0.237	0.260	0.232	0.241
3	0.238	0.250	0.232	0.239
4	0.248	0.251	0.231	0.239
5	0.245	0.248	0.238	0.238
6	0.243	0.250	0.239	0.242
7	0.245	0.246	0.238	0.239
8	0.242	0.245	0.232	0.237
9	0.239	0.245	0.226	0.239
10	0.242	0.245	0.239	0.239
11	0.244	0.250	0.239	0.238
12	0.241	0.251	0.237	0.241
Average	0.242	0.249	0.235	0.239
std. dev.	0.003	0.004	0.004	0.003

[a] Via analysis of $H_{Ar,G}$. [b] Via analysis of $H_{Ar,H}$. [c] Via analysis of H_1. [d] Via analysis of H_γ.

Table 5. Fraction of host occupied by guest (θ) for five independent Fourier transformations $[\mathbf{1}]_0 = [\mathbf{2}\text{-TFA}]_0 = 4.00$ mM, $CDCl_3/CD_3CN$ (3:2), 295 K.

Trial	$\theta^{[a]}$	$\theta^{[b]}$	$\theta^{[c]}$	$\theta^{[d]}$
1	0.241	0.251	0.237	0.241
2	0.244	0.252	0.235	0.242
3	0.242	0.253	0.236	0.243
4	0.244	0.251	0.239	0.242
5	0.243	0.252	0.236	0.242
average	0.243	0.252	0.237	0.242
std. dev.	0.001	0.001	0.001	0.001

[a] Via analysis of $H_{Ar,G}$. [b] Via analysis of $H_{Ar,H}$. [c] Via analysis of H_1. [d] Via analysis of H_γ.

We factored into our calculations errors from solution preparation and NMR integration. For integration errors, we allowed a standard deviation of ±2% in the calculated percentage of complexed **1**, which overestimates the true errors as determined from Tables 3 and 4. These errors were then followed through all calculations. For analysis, data points above 90% and below 10% complexed were ignored.[14] Linear regressions were performed using the entire error range (abscissa and ordinate) at each data point; standard errors in both the intercept and slopes based on regression were used to determine errors in K_{a5} and K_{ipd}, as shown in Table 1.

Acknowledgements

The authors are grateful to the NSF (grants DMR-0097126 and DMR-0704076) for support of this work. J.W.J. acknowledges support from the Environmental Management Science Program, Office of Science, US Department of Energy, through the Higher Education Research Experience (HERE) at Oak Ridge National Laboratory. We are grateful to the National Science Foundation for funds to purchase the Varian Unity Plus NMR (DMR-8809714) and the Varian Inova NMR (CHE-0131124) instruments, and the single-crystal X-ray diffractometer (CHE-0131128).

[1] a) D. J. Cram, J. M. Cram, *Container Molecules and Their Guests* (Ed.: J. F. Stoddart), RSC, Cambridge, **1994**; b) J.-M. Lehn, *Supramolecular Chemistry*, VCH, Weinheim, **1995**; c) P. D. Beer, P. A. Gale, D. K. Smith, *Supramolecular Chemistry*, Oxford University Press, Oxford, **1999**; d) J. W. Steed, J. L. Atwood, *Supramolecular Chemistry*, Wiley, New York, **2000**; e) L. F. Lindoy, I. M. Atkinson, *Self-Assembly in Supramolecular Systems* (Ed.: J. F. Stoddart), RSC, Cambridge, **2000**; f) *Core Concepts in Supramolecular Chemistry and Nanochemistry* (Eds.: J. W. Steed, D. R. Turner, K. J. Wallace), Wiley, New York, **2007**; g) P. A. Gale, *Royal Soc. Ser. Adv. Sci.* **2007**, *3*, 105–125; h) *Supramolecular Chemistry*, 2nd ed. (Eds.: J. W. Steed, J. L. Atwood), Wiley, New York, **2009**.

[2] See, for example: a) B. C. Bunker, D. L. Huber, J. G. Kushmerick, T. Dunbar, M. Kelly, C. Matzke, J. Cao, J. O. Jeppesen, J. Perkins, A. H. Flood, J. F. Stoddart, *Langmuir* **2007**, *23*, 31–34; b) Y. Liang, H. Wang, S. Yuan, Y. Lee, L. Gan, L. Yu, *J. Mater. Chem.* **2007**, *17*, 2183–2194; c) M. A. Palacios, R. Nishiyabu, M. Marquez, P. Anzenbacher, Jr., *J. Am. Chem. Soc.* **2007**, *129*, 7538–7544; d) E. R. Kay, D. A. Leigh, F. Zerbetto, *Angew. Chem.* **2007**, *119*, 72–196; *Angew. Chem. Int. Ed.* **2007**, *46*, 72–191; e) T. Ogoshi, A. Harada, *Sensors* **2008**, *8*, 4961–4982; f) X. Y. Ling, D. N. Reinhoudt, J. Huskens, *Pure Appl. Chem.* **2009**, *81*, 2225–2233; g) D. Li, W. F. Paxton, R. H. Baughman, T. J. Huang, J. F. Stoddart, P. S. Weiss, *Mater. Res. Soc. Bull.* **2009**, *34*, 671–681; h) H.-J. Schneider, R. M. Strongin, *Acc. Chem. Res.* **2009**, *42*, 1489–1500; i) V. Balzani, A. Credi, M. Venturi, *Chem. Soc. Rev.* **2009**, *38*, 1542–1550; j) M. A. Olson, A. B. Braunschweig, L. Fang, T. Ikeda, R. Klajn, A. Trabolsi, P. J. Wesson, D. Benitez, C. A. Mirkin, B. A. Grzybowski, J. F. Stoddart, *Angew. Chem.* **2009**, *121*, 1824–1829; *Angew. Chem. Int. Ed.* **2009**, *48*, 1792–1797; k) J. R. Kumpfer, J. Jin, S. J. Rowan, *J. Mater. Chem.* **2010**, *20*, 145–151; l) V. Palermo, E. Schwartz, C. E. Finlayson, A. Liscio, M. B. J. Otten, S. Trapani, K. Muellen, D. Beljonne, R. H. Friend, R. J. M. Nolte, A. E. Rowan, P. Samori, *Adv. Mater.* **2010**, *22*, E81–E88; m) L. A. Baumes, M. Buaki Sogo, P. Montes-Navajas, A. Corma, H. Garcia, *Chem. Eur. J.* **2010**, *16*, 4489–4495; n) Q. Zhang, Y. Tu, H. Tian, Y.-L. Zhao, J. F. Stoddart, H. Agren, *J. Phys. Chem. B* **2010**, *114*, 6561–6566.

[3] C. J. Pedersen, *J. Am. Chem. Soc.* **1967**, *89*, 7017–7036.

[4] E. A. Katayev, P. J. Melfi, J. L. Sessler in *Modern Supramolecular Chemistry* (Eds.: F. Diederich, P. J. Stang, R. R. Tykwinski), Wiley-VCH, Weinheim, **2008**, pp. 315–347.

[5] A. Spaeth, B. Koenig, *Beilstein J. Org. Chem.* **2010**, *6*, No. 32.

[6] a) R. H. Griffey, *Chem. Biol.* **2002**, *9*, 958–959; b) K. Hirose, *J. Inclusion Phenom. Macrocyclic Chem.* **2001**, *39*, 193–209; c) K. L. Rundlett, D. W. Armstrong, *Electrophoresis* **2001**, *22*, 1419–1427; d) L. Fielding, *Tetrahedron* **2000**, *56*, 6151–6170; e) K. A. Connors, *Binding Constants*, Wiley, New York, **1997**.

[7] a) R. M. Fuoss, *J. Am. Chem. Soc.* **1958**, *80*, 5050–5061; b) N. Isaacs, *Physical Organic Chemistry*, 2nd ed., Longmans, London, **1995**, pp. 56–62.

[8] The following examples considered ion pairing issues: a) C. Cambillau, G. Bram, J. Corset, C. Riche, *Can. J. Chem.* **1982**, *60*, 2554–2565; b) C. Chen, W. Wallace, E. M. Eyring, S. Petrucci, *J. Phys. Chem.* **1984**, *88*, 5445–5450; c) L Tusek-Bozic, *Electrochim. Acta* **1994**, *39*, 471–473; d) A. D′Aprano, B. Sesta, V. Mauro, M. J. Salomon, *J. Inclusion Phenom. Macrocyclic Chem.* **1999**, *35*, 451–465; e) H. J. Buschmann, G. W. Schollmeyer, *Inorg. Chem. Commun.* **2001**, 53–56; f) J. M. Mahoney, J. P. Davis, A. M. Beatty, B. D. Smith, *J. Org. Chem.* **2003**, *68*, 9819–9820; g) T. Yamamoto, A. M. Arif, P. J. Stang, *J. Am. Chem. Soc.* **2003**, *125*, 12309–12317; h) F. Arnaud-Neu, R. Delgado, S. Chaves, *Pure Appl. Chem.* **2003**, *75*, 71–102; i) F. Huang, J. W. Jones, H. W. Gibson, *J. Am. Chem. Soc.* **2003**, *125*, 14458–14464; j) F. P. Schmidtchen, *Coord. Chem. Rev.* **2006**, *250*, 2918–2928; k) T. B. Gasa, J. M. Spruell, W. R. Dichtel, T. J. Sorensen, D. Philp, J. F. Stoddart, P. Kuzmic, *Chem. Eur. J.* **2009**, *15*, 106–116; l) C. Roelens, A. Vacca, C. Venturi, *Chem. Eur. J.* **2009**, *15*, 2635–2644; m) S. Kubik, *Chem. Soc. Rev.* **2009**, *38*, 585–605; n) M. Semeraro, A. Arduini, M. Baroncini, R. Battelli, A. Credi, M. Venturi, A. Pochini, A. Secchi, S. Silvi, *Chem. Eur. J.* **2010**, *16*, 3467–3475.

[9] For reviews of pseudorotaxanes, related rotaxanes and catenanes and polymeric analogues, see: a) *Molecular Catenanes, Rotaxanes and Knots* (Eds.: J.-P. Sauvage, C. O. Dietrich-Buchecker), Wiley-VCH, Weinheim, **1999**; b) E. Mahan, H. W. Gibson in *Cyclic Polymers*, 2nd ed. (Ed.. J. A. Semlyen), Kluewer Publishers, Dordrecht, **2000**, pp. 415–560; c) T. J. Hubin, D. H. Busch, *Coord. Chem. Rev.* **2000**, *200–202*, 5–52; d) I. G. Panova, I. N. Topchieva, *Russ. Chem. Rev.* **2001**, *70*, 23–44; e) T. Takata, N. Kihara, Y. Furusho, *Adv. Polym. Sci.* **2004**, *171*, 1–75; f) F. Huang, H. W. Gibson, *Prog. Polym. Sci.* **2005**, *30*, 982–1018; g) G. Wenz, B.-H. Han, A. Mueller, *Chem. Rev.* **2006**, *106*, 782–817; h) M. D. Lankshear, P. D. Beer, *Acc. Chem. Res.* **2007**, *40*, 657–668; i) S. Loethen, J.-M. Kim, D. H. Thompson, *Polym. Rev.* **2007**, *47*, 383–418; j) J. J. Gassensmith, J. M. Baumes, B. D. Smith, *Chem. Commun.* **2009**, 6329–6338; k) J. F. Stoddart, *Chem. Soc. Rev.* **2009**, *38*, 1802–1820; l) J. D. Crowley, S. M. Goldup, A.-L. Lee, D. A. Leigh, R. T. McBurney, *Chem. Soc. Rev.* **2009**, *38*, 1530–1541; m) A. Harada, A. Hashidzume, H. Yamaguchi, Y. Takashima, *Chem. Rev.* **2009**, *109*, 5974–6023; n) N. Yui, R. Katoono, A. Yamashita, *Adv. Polym. Sci.* **2009**, *222*, 55–77; o) L. Fang, M. A. Olson, D. Benitez, E. Tkatchouk, W. A. Goddard III, J. F. Stoddart, *Chem. Soc. Rev.* **2010**, *39*, 17–29.

[10] M. C. T. Fyfe, J. F. Stoddart, *Adv. Supramol. Chem.* **1999**, *6*, 1–53.

[11] J. W. Jones, H. W. Gibson, *J. Am. Chem. Soc.* **2003**, *125*, 7001–7004.

[12] a) H. W. Gibson, N. Yamaguchi, L. Hamilton, J. W. Jones, *J. Am. Chem. Soc.* **2002**, *124*, 4653–4665; b) P. R. Ashton, R. Ballardini, V. Balzani, M. Gómez-López, S. E. Lawrence, M. V. Martínzez-Díaz, M. Montalti, A. Piersanti, L. Prodi, J. F. Stoddart, D. J. Williams, *J. Am. Chem. Soc.* **1997**, *119*, 10641–10651.

[13] Kochi has shown the parallel between ion pairing behavior in solution and in the solid state. [a) M. G. Davlieva, J.-M. Lü, S. V. Lindeman, J. Kochi, *J. Am. Chem. Soc.* **2004**, *126*, 4557–4565] On the basis of the large separations between the anions and the cations, X-ray crystal structures demonstrate non-ion paired inclusion complexes of DB24C8 (**1**) with NH_4PF_6 [b) G. D. Fallon, V. L. Lau, S. J. Langford, *Acta Crystallogr. Sect. E* **2002**, *58*, o321–o323], with **2**-PF_6 [c) P. R. Ashton, P. J. Campbell, E. J. T. Chrystal, P. T. Glink, S. Menzer, D. Philp, N. Spencer, J. F. Stoddart, P. A. Tasker, D. J. Williams, *Angew. Chem.* **1995**, *107*, 1997–2001; *Angew. Chem. Int. Ed. Engl.* **1995**, *34*, 1865–1869. [We also obtained this structure; see the Supporting Information], both with bis(*p*-chlorobenzyl)ammonium PF_6 and bis(*m*-nitrobenzyl)ammonium PF_6 [d) P. R. Ashton, M. C. T. Fyfe, S. K. Hickingbottom, J. F. Stoddart, A. J. P. White, D. J. Williams, *J. Chem. Soc. Perkin Trans. 2* **1998**, 2117–2128] and with bis(*o*-methylbenzyl)ammonium PF_6 [e) H. W. Gibson, N. Yamaguchi, Z. Niu, J. W. Jones, A. L. Rheingold, L. N. Zakharov, *J. Polym. Sci. Part A Polym. Chem. Ed.* **2010**, *48*, 975–985]; likewise, the solid-state complex of **2**-PF_6 with *anti*- bis(carbomethoxy)dibenzo-[30]crown-10 is not ion paired [f) H. W. Gibson, H. Wang, K. Bonrad, J. W. Jones, C. Slebodnick, B. Habenicht, P. Lobue, *Org. Biomol. Chem.* **2005**, *3*, 2114–2121].

[14] G. Weber, *Molecular Biophysics* (Eds.: B. Pullman, M. Weissbluth), Academic Press, New York, **1965**, pp. 369–397.

[15] P. R. Ashton, E. J. T. Chrystal, P. T. Glink, S. Menzer, C. Schiavo, N. Spencer, J. F. Stoddart, P. A. Tasker, A. J. P. White, D. J. Williams, *Chem. Eur. J.* **1996**, *2*, 709–728.

[16] T. Akai, N. Nakamura, H. Chihara, *J. Chem. Soc. Faraday Trans.* **1993**, *89*, 1339–1343.

[17] J. W. Jones, F. Huang, W. S Bryant, H. W. Gibson, *Tetrahedron Lett.* **2004**, *45*, 5961–5963.

[18] M. Montalti, L. Prodi, *Chem. Commun.* **1998**, 1461–1462.

[19] For related pre-equilibrium schemes, see: a) H. Farber, S. Petrucci, *J. Phys. Chem.* **1981**, *85*, 1396–1401 and b) H. Richman, Y. Harada, E. M. Eyring, S. Petrucci, *J. Phys. Chem.* **1985**, *89*, 2373–2376.

[20] a) G. N. Lewis, M. Randall, *J. Am. Chem. Soc.* **1921**, *43*, 1112–1154; b) P. Debye, E. Hückel, *Z. Phys.* **1923**, *24*, 305–325.

[21] D. G. Lide, *CRC Handbook of Chemistry and Physics*, 76th ed., Chemical Rubber Co., Boca Raton, **1995**.

[22] For R_4NX (R = Me, *n*Pr, *n*Bu, *i*Am; X = PF_6, $B(C_6H_5)_4$, ClO_4, Cl, SCN) in CH_3CN $K_{ipd} = 2–4 \times 10^{-2}$ M [a) J. Barthel, L. Iberl, J. Rossmaier, H. J. Gores, B. Kaukal, *J. Solution Chem.* **1990**, *19*, 321–337], in acetone $K_{ipd} = 1–3 \times 10^{-3}$ M [b) L. G. Savedoff, *J. Am. Chem. Soc.* **1966**, *88*, 664–667] and in CH_2Cl_2 $K_{ipd} = 1 \times 10^{-4}$ to 5×10^{-5} M [c) R. Romeo, G. Arena, L. M. Scolaro, M. R. Plutino, *Inorg. Chim. Acta* **1995**, *240*, 81–92. For TBA-PF_6 K_{ipd} is reported as follows: in THF 2.68×10^{-6} M [d) R. J. LeSeur, C. Buttolph, W. E. Geiger, *Anal. Chem.* **2004**, *76*, 6395–6401], 1.42×10^{-4} M [e) N. G. Tsierkezos, A. I. Philippopoulos, *Fluid Phase Equilib.* **2009**, *277*, 20–28]; in CH_3CN 2.80×10^{-2} M [reference [22d]], 1.10×10^{-2} M [reference [22e]]; in CH_2Cl_2 6.47×10^{-4} M [reference [22e]].

[23] a) R. Schmid, K. Kirchner, F. L. Dickert, *Inorg. Chem.* **1988**, *27*, 1530–1536; b) S. F. Nelsen, R. F. Ismagilov, *J. Phys. Chem. A* **1999**, *103*, 5373–5378.

[24] M. Born, *Z. Phys.* **1920**, *1*, 45–48.

[25] a) R. Haque, W. R. Coshow, L. F. Johnson, *J. Am. Chem. Soc.* **1969**, *91*, 3822–3827; b) R. L. Buckson, S. G. Smith, *J. Phys. Chem.* **1964**, *68*, 1875–1878; c) R. C. Neuman Jr. , V. Jonas, *J. Phys. Chem.* **1971**, *75*, 3550–3554; d) Y.-Y. Lim, R. Drago, *J. Am. Chem. Soc.* **1972**, *94*, 84–90; e) S. Khazaeli, A. I. Popov, J. L. Dye, *J. Phys. Chem.* **1982**, *86*, 4238–4244; f) P. Haake, R. Prigodich, *Inorg. Chem.* **1984**, *23*, 457–462.

[26] a) R. M. Fuoss, C. A. Kraus, *J. Am. Chem. Soc.* **1933**, *55*, 2387–2399; b) Z. Chen, M. Hojo, *J. Phys. Chem. B* **1997**, *101*, 10896–10902; c) M. Hojo, T. Ueda, M. Nishimura, H. Hamada, M. Matsui, S. Umetani, *J. Phys. Chem. B* **1999**, *103*, 8965–8972; d) M. Hojo, *Pure Appl. Chem.* **2008**, *80*, 1539–1560.

[27] a) L. Brunsveld, B. J. B. Folmer, E. W. Meijer, R. P. Sijbesma, *Chem. Rev.* **2001**, *101*, 4071–4097; b) H. W. Gibson, N. Yamaguchi, J. W. Jones, *J. Am. Chem. Soc.* **2003**, *125*, 3522–3533; c) F. Huang, D. S. Nagvekar, X. Zhou, H. W. Gibson, *Macromolecules* **2007**, *40*, 3561–3567; d) F. Wang, J. Zhang, X. Ding, S. Dong, M. Liu, B. Zheng, S. Li, L. Wu, Y. Yu, H. W. Gibson, F. Huang, *Angew. Chem.* **2010**, *122*, 1108–1112; *Angew. Chem. Int. Ed.* **2010**, *49*, 1090–1094.

[28] H. W. Gibson, Z. Ge, F. Huang, J. W. Jones, H. Lefebvre, M. J. Vergne, D. M. Hercules, *Macromolecules* **2005**, *38*, 2626–2637.

[29] We recognize the advantage to be gained in studying complexation in the low concentration regime by fluorescence spectroscopy, but found that the emission spectra for **1** and **2**-X overlap, **1** yielding $\lambda_{em\,max} = 410$ nm, and **2**-PF_6 yielding a broad emission band from 370 to >500 nm, with $\lambda_{em\,max} = 425$ nm. The excitation spectra also over-

lap, **1** displaying $\lambda_{exmax}=277$ nm, and **2**-PF_6 yielding a broad excitation band from 260 to 400 nm.
[30] See: *ChemTech* **1986**, *16*, 177.
[31] a) K. Zhu, M. Zhang, F. Wang, N. Li, S. Li, F. Huang, *New J. Chem.* **2008**, *32*, 1827–1830; b) K. Zhu, S. Li, F. Wang, F. Huang, *J. Org. Chem.* **2009**, *74*, 1322–1328; c) S.-K. Kim, J. L. Sessler, *Chem. Soc. Rev.* **2010**, *39*, 3784–3809.
[32] W. S. Bryant, PhD Thesis, Virginia Polytechnic Institute and State University (USA), **1999**.
[33] K. S. Mohamed, Padma, D. K. Indian, *J. Chem. Sect. A Inorg. Phys. Theor. Anal.* **1998**, *27A*, 759–763.
[34] CrysAlis CCD and CrysAlis RED, Oxford Diffraction Ltd., **2002**.
[35] SHELX-97 Program, G. M. Sheldrick, University of Göttingen (Germany), **1997**.

Received: September 1, 2010
Published online: February 9, 2011

